Materials Research Proceedings **25** (2023) 463-470 https://doi.org/10.21741/9781644902417-57

Investigation on the inter-ply friction when deforming magnesium-based fibre metal laminates at elevated temperature

Zheng Liu[1,a *], Enrico Simonetto[1,b], Andrea Ghiotti[1,c], Stefania Bruschi[1,d]

[1]Department of Industrial Engineering, University of Padova, Via Venezia 1, 35131 Padova, Italy

[a]zheng.liu@studenti.unipd.it, [b]enrico.simonetto.1@unipd.it, [c]andrea.ghiotti@unipd.it, [d]stefania.bruschi@unipd.it

Keywords: Friction, Hot Stamping, Fibre Metal Laminates

Abstract. Inter-ply friction plays a dominant role in inducing defects (e.g., wrinkling) during the hot stamping process of fibre metal laminates (FMLs). In particular, the metal/prepreg inter-ply friction is highly affected by the process parameters at elevated temperature as the molten matrix is significantly sensitive to possible changes in these parameters. In this paper, the metal/prepreg inter-ply friction was experimentally investigated at increasing relative sliding displacement and varying normal pressure. To do that, pull-through tests with a stop-start control strategy were conducted at elevated temperature. The obtained results showed the transition of the lubrication mode given by the Stribeck theory from a hydrodynamic to a mixed one as the relative sliding displacement rose at whatever normal pressure level. An increase in the inter-ply friction coefficient was found as well.

Introduction

Fibre metal laminates (FMLs), a form of hybrid laminated material system made up of thin metal sheets laminated with fibre-reinforced polymer (FRP) layers, take advantage of both the material categories, as they overcome the FRP reduced toughness, and, at the same, enhance the mechanical resistance of monolithic metal sheets [1]. Aluminium alloy-based FMLs, such as glass-reinforced aluminium laminates (GLARE), aramid-reinforced aluminium laminates (ARALL), and carbon-reinforced aluminium laminates (CARALL), were introduced in the aerospace sector to reduce the overall weight and improve the impact and fatigue responses of structural parts [2]. Recently, driven by the increasing demand for high strength-to-density parts, magnesium alloy-based FMLs have been introduced, with also the chance of widening the FMLs applications thanks to the effective electromagnetic interference shielding offered when magnesium alloy sheets are used [3].

For the composite core, there has been a rise in the adoption of continuous carbon fibre reinforced thermosetting polymers (CFRPs) for structural applications. Nevertheless, since thermoplastic polymers guarantee reduced cycle time, recyclability, and better compatibility with the currently available stamping lines [4], they are becoming an alternative to thermosetting ones as matrices of the composite core. However, thermoplastic polymers have a significantly higher melting viscosity than thermosetting ones, bringing various issues during the forming process that may affect the part final performances. FMLs are usually formed at elevated temperature to take advantage of the metal sheet higher formability. The deformation mechanisms taking place during stamping at elevated temperature mainly include intra-ply behaviours such as in-plane shear, out-plane bending, tension, transverse compression, and inter-ply behaviours consisting of ply/tool and ply/ply slippage [5]. In particular, the inter-ply friction is relevant to both the interface between two plies of the composite and the interface between the metal sheet and the composite. The inter-ply friction may have a significant impact on the onset of defects, such as wrinkling, during stamping, and can lead to undesired changes in the yarns, which, in turn, can lead to fibre in-plane undulations or in-plane waviness in the formed parts. Numerous researchers have investigated how process parameters such as the normal pressure, sliding velocity, and temperature may affect the tool/ prepreg inter-ply friction in case of hot stamping FRPs within the hydrodynamic lubrication range, and the obtained results were consistent with the Stribeck theory, which states that the kinetic friction coefficient can be linearly fitted as a function of the Hersey number, which is determined by the normal pressure (p), the viscosity of the liquid(η) and the relative sliding velocity(v), as shown in Fig. 1 from the work of Gorczyca-Cole et al. [6]. Chow [7] performed experiments to analyse the inter-ply friction of commingled glass polypropylene four-harness satin-weave fabric between the binder ring and the die: the mixed lubrication mode was found in this research, and an inter-ply friction analytical model was introduced accordingly to incorporate the weighted effects of the Coulomb and hydrodynamic friction models at varying process parameters. To measure the kinetic friction, Sachs et al. [8] compared and reviewed various friction test setups in terms of their measured coefficients of friction using a standardization procedure.

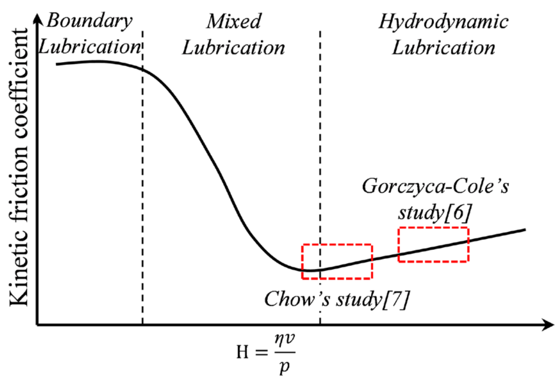

Fig. 1 Stribeck curve: kinetic friction coefficient versus Hersey number.

During the forming process carried out at temperature above the melting one of the thermoplastic polymer matrix of the composite, the thickness of the resin between the metal and composite layers varies as a consequence of the gradient of the normal pressure applied on the metal layers and the metal/composite inter-ply slippage. From the tribological viewpoint, the distance between two solid surfaces separated by a thin liquid film significantly affects the solid/liquid interfacial shear stress and further influences their inter-ply friction [9]. In this framework, in order to gain a comprehensive understanding of the mechanisms in the hot stamping process of magnesium alloy-based FMLs, the effect of the normal pressure on the inter-ply friction was investigated, as well as the coupled effect of the normal pressure and relative sliding displacement was studied.

Materials and Methods

Materials. The FMLs investigated in this study are made of glass fibre-reinforced PA6 prepregs (Tepex® 102-RG600 (2)/47% Type B, thickness 1 mm) and AZ31B magnesium alloy sheets (thickness 0.5 mm) arranged as described below. The mechanical characteristics of the magnesium alloy sheets and prepregs in the as-delivered condition were evaluated by carrying out standard tensile tests (ISO-6892) on a 50 kN MTS™ 322 hydraulic dynamometer, as shown in Table 1. The main characteristics of the prepregs are presented in Table 2.

Table 1 Mechanical properties of the AZ31B sheets and prepregs.

AZ31B sheets		Prepregs	
Elastic Modulus	45 GPa	Tensile modulus	18 GPa
Yield Strength	158±2 MPa	Tensile strength	380±5 MPa
Tensile Strength	248±4 MPa	Strain at break	2.3%
Shear Modulus	16.7 GPa	Flexural Modulus	16 GPa
Poisson's Ratio	0.35	Flexural Strength	300 ±5 MPa

Materials Research Proceedings **25** (2023) 463-470 https://doi.org/10.21741/9781644902417-57

Table 2 Main characteristics of the prepregs [10].

Layup	Value		Unit
	Longitudinal	Transversal	
Fibre	E-Glass		
Weaving style	Twill 2/2		
Area weight (dry fabric)	600		g/m²
Yarn count	1200		tex
Yarn density	2.5	2.5	1/cm
Weight rate	50	50	%
Fibre content	47		Vol-%
Thickness per layer	0.5		mm
Laminate density	1.8		g/cm³

Stop-start pull-through tests. According to the ASTM standard D3528 [11] for evaluating the tensile and shear strengths of adhesives for bonding metals, the testing apparatus shown in Fig. 2 (a) and (b) was designed and constructed for the measurement of the metal/prepreg inter-ply friction coefficient. The adopted cross-shaped specimen is made of two prepreg layers along the horizontal direction and one metal sheet between them along the vertical direction (see Fig. 3 for the sketch and dimensions of the specimen). The specimens were tested in a plate-plate configuration with a constant overlapping area of 20 x 20 mm^2, see Fig. 3. The tests were performed on the MTS™ 322 hydraulic dynamometer equipped with the MTS™ 651 environmental chamber to heat up the specimen to the testing temperature. To achieve a uniform temperature distribution, the set-up was heated up for 1 hour before assembling the specimen. The metal sheet was gripped to the lower clamp of the testing machine so that the pulling velocity could be controlled. Various normal forces F were adopted by controlling the stroke of the compression spring shown in Fig. 2. Therefore, the normal pressure p can be calculated from Eq. 1, where A is the overlapping area shown in Fig. 3. The homogeneous normal pressure distribution is assumed in this research. With the normal pressure applied on this area, the concave and convex structures of the fibres will be easily flattened at elevated temperatures, which contributes to a neglectable nonuniform normal pressure distribution.

$$p = \frac{F}{A}. \tag{1}$$

To assess the potential effect of the metal/prepregs relative sliding displacement on the inter-ply friction, the total stroke of the magnesium alloy sheet along the pulling direction, namely 25 mm, was uniformly divided into 5 stages as indicated in Fig. 3. A stop-start control strategy was applied in each stage to obtain the inter-ply friction coefficient. Pulling-through of the AZ31B sheet was regulated in a distance-controlled mode within each stage, so that the test was conducted at a given sliding velocity, meanwhile, the pulling force was monitored as a function of the distance. The test was stopped for one minute at the end of each stage to relax and relieve the stress, and then restarted for the next stage.

The pull-through tests were conducted at normal pressure of 0.5 MPa, 2.5 MPa, and 5 MPa, which covers the range of normal pressure in the thermoforming process of typical hat-shaped FMLs with the same material system [12]. To investigate the effect of normal pressure on the inter-ply friction, other influence factors were kept constant with the pulling velocity of the AZ31B sheet fixed at 0.5 mm/s as well as the testing temperature at 235℃, which is above the PA6 melting temperature, namely 220℃. For each testing condition, five tests were performed to assure the repeatability of the results.

Materials Research Proceedings **25** (2023) 463-470 https://doi.org/10.21741/9781644902417-57

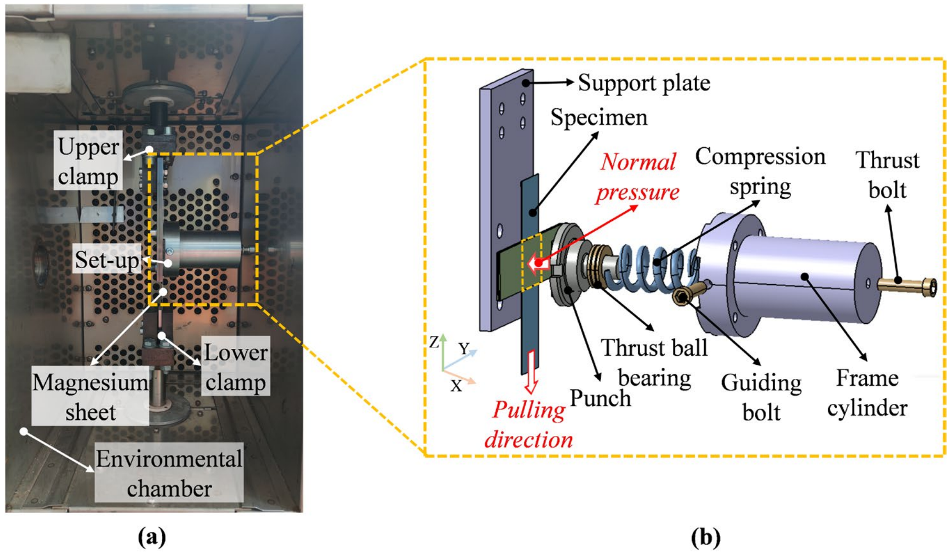

Fig. 2 Set-up for the stop-start pull-through tests: (a) assembly; (b) scheme.

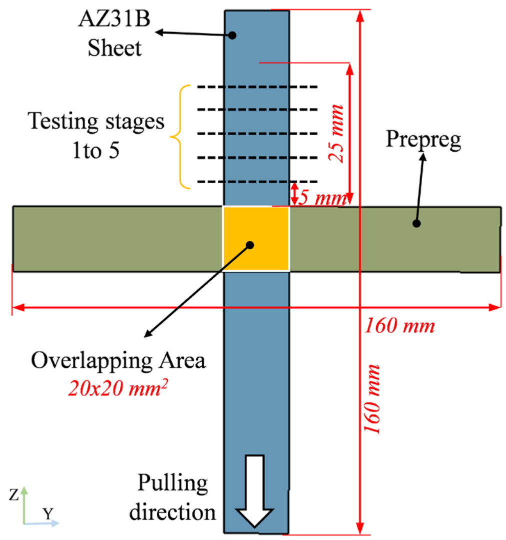

Fig. 3 Sketch and dimensions of the specimen used in the stop-start pull-through tests.

Test data elaboration. Fig. 4 illustrates the friction force developing between two surfaces separated by a liquid film. When the liquid film is thick enough, the friction force shows a typical liquid-like characteristic: it rises first at increasing relative sliding displacement, and then it reaches a stable value, named F_k, the kinetic friction force. As the liquid film thickness decreases, a hard-wall film occurs as a result of the increase in the liquid viscosity [13]. Therefore, a solid-like shear response is observed, characterized by the static friction force Fs.

The pulling force F measured during the stop-start pull-through tests, namely the friction force, can be used to calculate the inter-ply shear stress τ using Eq. 2.

$$\tau = \frac{F}{2A} \tag{2}$$

Furthermore, the static shear stress τ_S and kinetic shear stress τ_K can be obtained from Eq. 3 and Eq. 4, respectively.

$$\tau_S = \frac{F_S}{2A} \tag{3}$$

$$\tau_K = \frac{F_K}{2A} \tag{4}$$

Therefore, the static and kinetic friction coefficients can be calculated according to Eq. 5 and Eq. 6, respectively.

$$u_S = \frac{\tau_S}{p} \tag{5}$$

$$u_K = \frac{\tau_K}{p} \tag{6}$$

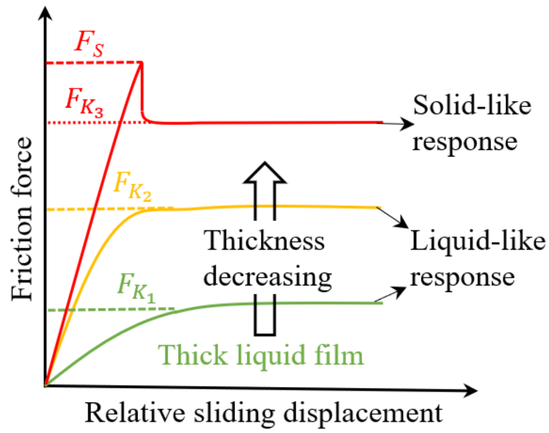

Fig. 4 Friction force between two surfaces separated by a liquid film.

Results and discussion

Influence of the relative sliding displacement on the inter-ply friction. Fig shows the inter-ply shear stress τ at different stages when applying 2.5 MPa as normal pressure p. It can be seen that the evolution of the shear stress is significantly different as the stage increases. A gradual increase in the shear stress followed by a steady state was found in case of the stages 1 and 2: this is indicative of a liquid-like inter-ply shear characteristic, which makes negligible the difference between the static and dynamic friction coefficients as shown in Fig. 5 (b) at these two stages. This can be further proved by the morphology of the residues on the surface of the tested magnesium alloy sheets (see Fig. 6). As most of the residues detected on the AZ31 sheets at stage 1 were of the polymer matrix, the inter-ply shear occurred at the interface between the metal and the polymer matrix. At the initial two stages, the molten polymer matrix actually worked as a sort of liquid lubricant at the metal/prepreg interface. As a result, the prepreg and the metal sheet were separated by a liquid film, which identifies the hydrodynamic mode of lubrication. From stages 1 to 2, more molten polymer matrix was removed from the connecting area due to the longer relative sliding displacement, and, as a consequence, the thickness of the polymer matrix becomes thinner. At stage 3, a mixture of polymer matrix and entangled fibres is visible on the tested magnesium alloy sheets as shown in Fig. 6 (b). This means that the mixed mode of the metal/polymer matrix and metal/fibre inter-ply friction makes the metal/prepreg inter-ply friction fall into the mixed lubrication range. A different shear stress response is also brought by the transition of the lubrication mode: the shear stress curve relevant to stage 3 in Fig. 5 (a), after reaching the peak point, decreases until a steady state level is reached. This curve clearly shows a solid-like inter-ply shear response. From stage 3 to stage 5, there is a growing divergence between the static and dynamic friction coefficients as shown in Fig. 5 (b). At stage 5, the difference reaches its maximum value, confirmed by the mixture of fibre and polymer matrix-dominate residues on the tested AZ31 sheets (see Fig. 6 (c)). What's more, the metal/fibre inter-ply friction coefficient, which can be interpreted as the Coulomb friction coefficient, is higher than the one at the metal/ polymer matrix interface, so the inter-ply friction coefficient increases at increasing fibre volume fraction. This explains why, as the stage moves from 3 to 5, both the inter-ply friction and shear stress rise. From stages 1 to 5, it can be seen that as the stage rose, the stroke reaching the shear stress peak declined. This can be explained by the fact that as the amount of molten polymer matrix in the contacting area reduces, the content of fibre grows, increasing the viscosity of the interface layer and further raising the system shear modulus (the ratio of the peak shear stress to the corresponding shear strain) [14].

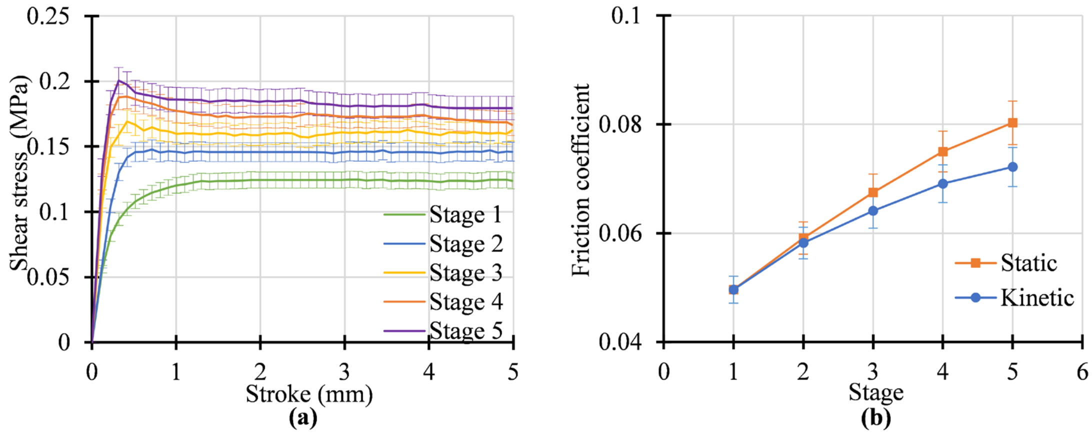

Fig. 5 Pull-through test results at different stages and 2.5 MPa normal pressure: (a) shear stress, and (b) friction coefficient.

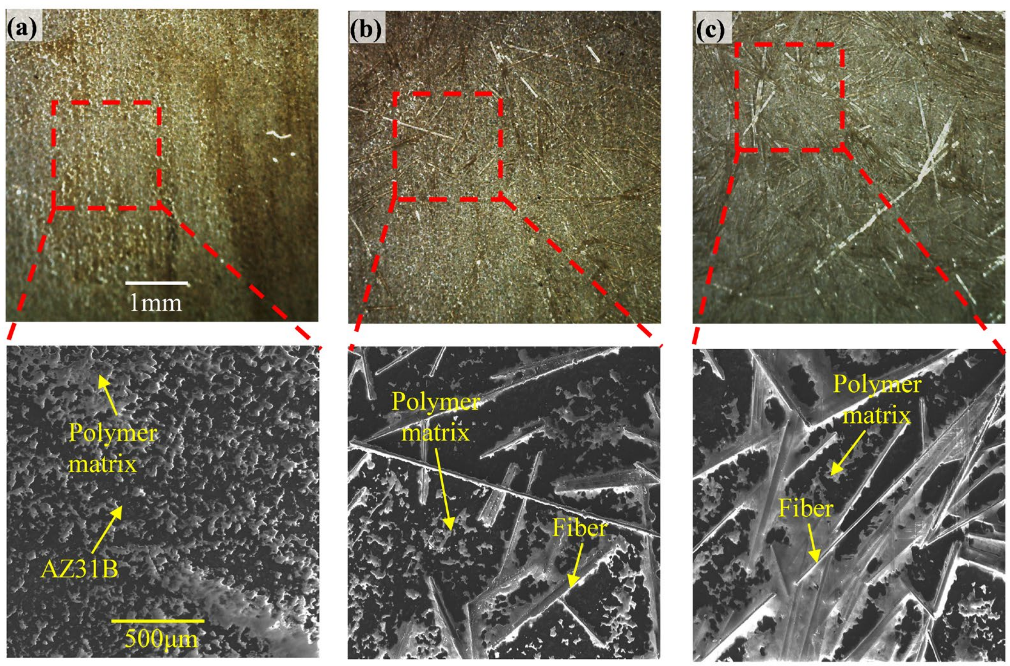

Fig. 6 Morphology of the residues on the tested AZ31 sheets at different stages:(a) stage 1, (b) stage 3, and (c) stage 5.

Influence of the normal pressure on the inter-ply friction. Fig. 7 shows the pull-through test results at varying normal pressure. As expected, from Fig. 7 (a), the higher the normal pressure (from 0.5 MPa to 5 MPa) the higher the shear stress (from $\tau^{p0.5}$ to τ^{p5}) at all the stages. However, the effect of increasing normal pressure on the increase in the inter-ply shear stress was less than linearly proportional. At stage 1, the liquid-like inter-ply friction at normal pressure from 0.5 MPa ($\mu^{p0.5}$) to 2.5 MPa ($\mu^{p2.5}$) made the inter-ply friction located in the hydrodynamic lubrication region. The net result was a decrease in the coefficient of friction at increasing normal pressure in this region, which is consistent with the results presented in [13]. This can be explained by the fact that the fibre layer was still characterized by a relatively rough surface when low values of the normal pressure were applied. On the contrary, the surface asperities were flattened at increasing normal pressure, which contributed to a decrease in the inter-ply friction coefficient. When the applied

Materials Research Proceedings **25** (2023) 463-470 https://doi.org/10.21741/9781644902417-57

normal pressure was 5 MPa, the surface of the fibre layer was further flattened, however, the mixed lubrication mode due to the direct contact between the metal sheet and fibre layer, as shown in Fig. 8 (a), increased the friction coefficient. As a result, the inter-ply friction at 5 MPa normal pressure was a little higher than that at 2.5 MPa. Moreover, the inter-ply shear stress as a function of the relative sliding displacement at varying normal pressure shows different tendencies. It can be seen that a solid-like shear response was found at stage 1 when the FML was subjected to a 5 MPa normal pressure, leading to fibre residues on the tested magnesium alloy sheet as shown in Fig. 8 (a). When the normal pressure was decreased to 2.5 MPa, the transition from a liquid-like response to a solid-like one was found at stage 3. For a normal pressure of 0.5 MPa, a slight gap between the static and kinetic shear stress between the metal and fibre layers was found at the last two stages. It can be seen that the highest normal pressure contributed to accelerate the transition from a liquid-like inter-ply friction response to a solid-like one. This can be explained by the fact that the higher the normal pressure the more the molten polymer matrix squeezed out from the contacting area, leading to a decrease in its thickness between the metal and the fibre layers at the initial stage. On the other hand, as the relative sliding displacement increased, the higher shear stress caused by the higher normal pressure aggravated the loss of resin. This phenomenon contributed to the contact between the fibre and metal layers. What's more, with the increasing contact area between the metal and fibre layers, a wider gap between the static and kinetic shear stresses was found at the highest normal pressure.

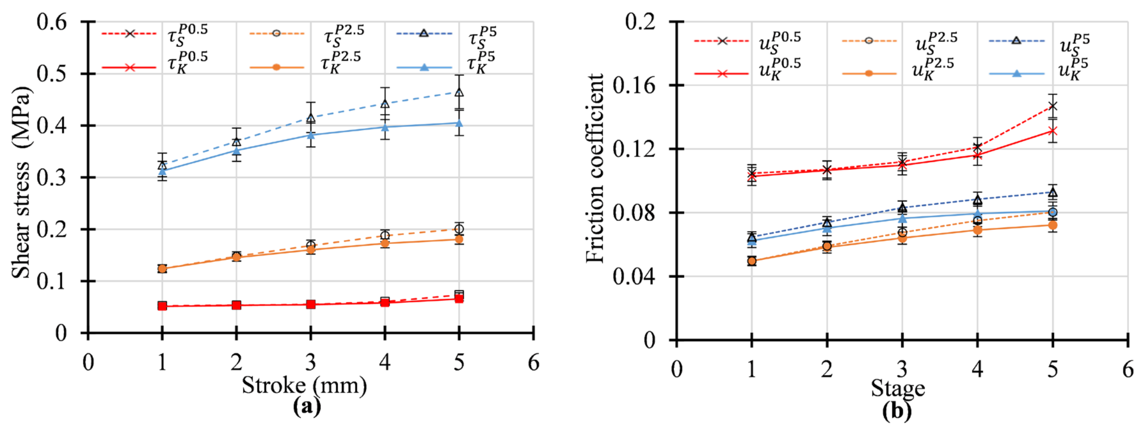

Fig. 7 Pull-through test results at varying normal pressure: (a) shear stress, and (b) friction coefficient.

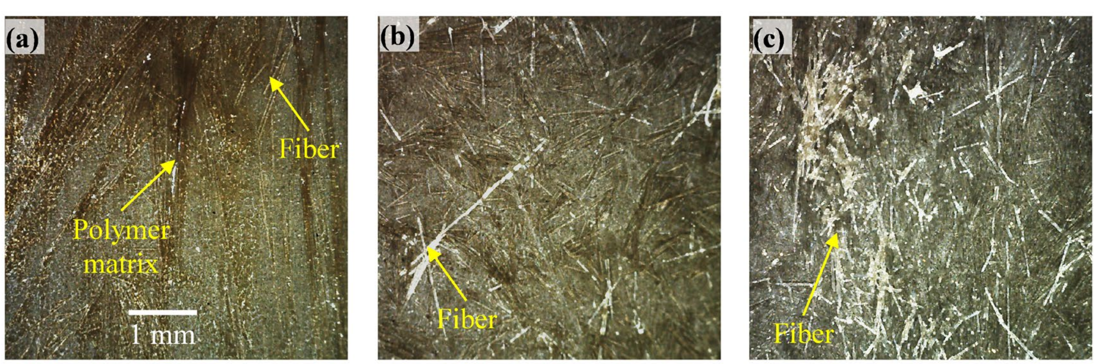

Fig. 8 Morphology of the residues on the tested AZ31 sheets at 5 MPa normal pressure: (a) stage 1, (b) stage 3, and (c) stage 5.

Summary

In this study, a comprehensive series of experiments were conducted to gain a better understanding of the effect of the normal pressure on the inter-ply friction when testing magnesium alloy-based

FMLs at elevated temperature. The main findings of the present research work can be summarized as follows. The metal/prepreg inter-ply friction at elevated temperature was found to be sensitive to the relative sliding displacement regardless of the applied normal pressure. As the relative sliding displacement rose, a transition from hydrodynamic lubrication mode to a mixed one was found, together with an increase of the inter-ply friction. Moreover, the increase in the normal pressure promoted the transition, further impacting the inter-ply friction.

References

[1] G. Lange, A. Carradò, H. Palkowski, Tailored sandwich structures in the focus of research, Mater Manuf Processes. 24 (2009):1150–4. https://doi.org/10.1080/10426910902978977

[2] X. Zhang, Q. Ma, Y. Dai, et al, Effects of surface treatments and bonding types on the interfacial behavior of fiber metal laminate based on magnesium alloy, Appl Surf Sci. 427 (2018) 897–906. https://doi.org/10.1016/j.apsusc.2017.09.024

[3] G. Lawcock, L. Ye, Y.W. Mai, C.Sun, The effect of adhesive bonding between aluminum and composite prepreg on the mechanical properties of carbon-fiber-reinforced metal laminates, Compos Sci Technol.57 (1997) 35–45. https://doi.org/10.1016/S0266-3538(96)00107-8

[4] H.M. El-Dessouky, CA. Lawrence, Ultra-lightweight carbon fibre/thermoplastic composite material using spread tow technology, Compos B Eng. 50 (2013) 91–97. https://doi.org/10.1016/j.compositesb.2013.01.026

[5] H. Chen, S. Li, J. Wang, A. Ding, A focused review on the thermo-stamping process and simulation, Composites Part B 224 (2021) 109196. https://doi.org/10.1016/j.compositesb.2021.109196

[6] J. L. Gorczyca-Cole, J. A. Sherwood, J.Chen A friction model for thermostamping commingled glass–polypropylene woven fabrics. Compos. Part A Appl. Sci. Manuf. 38 (2007) 393https://doi.org/10.1016/j.compositesa.2006.03.006

[7] S. Chow, Frictional interaction between blank holder and fabric in stamping of woven thermoplastic composites, Master thesis, Department of Mechanical Engineering, University of Massachusetts Lowell, 2002.

[8] U. Sachsa, R. Akkermanab, K. Fetfatsidisc, E. Vidal-Salléd, J.Schumachere, G. Ziegmanne, S. Allaouif, G. Hivetf, B. Marong, K. Vanclloosterh, S. V.Lomov, Characterization of the dynamic friction of woven fabrics: Experimental methods and benchmark results, Compos. Part A Appl. Sci. Manuf. 67 (2014) 289–298. https://doi.org/10.1016/j.compositesa.2014.08.026

[9] S. Yamada, Nanotribology of Symmetric and Asymmetric Liquid Lubricants, Symmetry. 2 (2010) 320-345. https://doi.org/10.3390/sym2010320

[10] Information on www.tepx.com.

[11] ASTM D1894, Standard test method for static and kinetic coefficients of friction of plastic film and sheeting. Annu. B. ASTM Standard International.

[12] Ghiotti, A., Bruschi, S., Kain, M., Lizzul, L., Simonetto, E., et al., Simultaneous bonding and forming of Mg fibre metal laminates at high temperature. J Manuf Process; 72:105-114. https://doi.org/10.1016/j.jmapro.2021.10.017

[13] L. Wang, P. Xu, X. Peng, K. Zhao, R. Wie, Characterization of inter-ply slipping behaviors in hot diaphragm preforming: Experiments and modelling, Compos. Part A Appl. Sci. Manuf. 121 (2019) 28–35. https://doi.org/10.1016/j.compositesa.2019.03.012

[14] S. Erland, T.J. Dodwell, R. Butler, Characterization of inter-ply shear in uncured carbon fibre prepreg, Compos. Part A Appl. Sci. Manuf .77 (2015) 210–218. https://doi.org/10.1016/j.compositesa.2015.07.008